



## Fusion Cross Section for Non-central Collision in $^{11}\text{Be} + ^{209}\text{Bi}$ Reaction using Multi-body Three-Stage Classical Molecular Dynamics Approach

V.B. Katariya<sup>1\*</sup> and P.H. Jariwala<sup>2</sup>

<sup>1</sup>Department of Physics, Veer Narmad South Gujarat University, Surat (Gujarat), India.

<sup>2</sup>Department of Physics, Navyug Science College, Surat (Gujarat), India.

(Corresponding author: V.B. Katariya\*)

(Received 04 February 2025, Revised 20 March 2025, Accepted 25 April 2025)

(Published by Research Trend, Website: [www.researchtrend.net](http://www.researchtrend.net))

DOI: <https://doi.org/10.65041/IJTAS.2025.17.1.14>

**ABSTRACT:** Halo nuclei shows unique structures that differ drastically from ordinary nuclear matter. Among these,  $^{11}\text{Be}$  is the most studied one and has gained great interest due to its well-established one-neutron halo structure and low neutron separation energy  $S_n = 0.501$  MeV. In this study, the fusion reaction  $^{11}\text{Be} + ^{209}\text{Bi}$  is investigated using the Multibody Three-stage Classical Molecular Dynamics (3S-CMD) model where  $^{11}\text{Be}$  is constructed as a cluster of tightly bound  $^{10}\text{Be}$  and one neutron where the separation between  $^{10}\text{Be}$  and neutron is adjusted to set the ion-ion potential between them equal to the experimental neutron separation energy. Complete fusion cross sections are calculated using Wong's formula. At higher energies, the contributions from higher partial waves become significant and cannot be ignored. To account this, the CF cross-section is calculated for non-central collisions ( $b > 0$ ) at critical impact parameter ( $b = b_{cr}$ ). This calculations reveal that fusion cross section for non-central collision at this critical impact parameter is enhanced.

**Keywords:** Heavy-ion Collisions, Classical Molecular Dynamics, Halo nuclei, Fusion cross-sections, Weakly bound nuclei.

### INTRODUCTION

Halo nuclei represent a class of nuclei that are radically different from normal nuclear matter. Several remarkable features were revealed in experiments (Tanihata *et al.*, 1985; Tanihata *et al.*, 1985; Kobayashi *et al.*, 1988; Kobayashi *et al.*, 1989) that were conducted to examine the properties of these so-called halo nuclei, including  $^8\text{He}$ ,  $^{11}\text{Li}$ ,  $^{11}\text{Be}$ ,  $^{14}\text{Be}$ ,  $^{17}\text{B}$ ,  $^{20}\text{C}$ , and  $^{22}\text{C}$ , among others which includes (i) abnormally large interaction cross sections, (ii) very weak binding of the outer few nucleons, which resulted in systems with qualitatively new structures and surface densities, and (iii) large dissociation cross sections of a halo nucleus by a high  $Z$ -target of a new exotic mode of collective vibrations in the nucleus. The advancements of experimental techniques and the availability of radioactive beam facilities have made it possible to study such nuclides near the limits of stability.

Among these halo nuclei,  $^{11}\text{Be}$  has gained considerable interest due to its well-established one-neutron halo structure. Its peculiar structure consists of a tightly bound  $^{10}\text{Be}$  core with a single valence neutron orbiting it. The low neutron separation energy ( $S_n = 0.501$  MeV)

(Signorini *et al.*, 2004) of  $^{11}\text{Be}$  significantly enhances the possibility of neutron knockout. Understanding the impact of such processes on fusion reactions is essential, as they influence the dynamics and outcomes of various reaction channels. These effects become particularly pronounced in reactions involving heavier targets such as  $^{209}\text{Bi}$ , where the long-range Coulomb interaction dominates over the nuclear potential (Duan *et al.*, 2020).

In the present work, the  $^{11}\text{Be} + ^{209}\text{Bi}$  reaction is studied using the Multibody Three-Stage Classical Molecular Dynamics (3S-CMD) model. Here,  $^{11}\text{Be}$  is constructed as a cluster comprising a tightly bound  $^{10}\text{Be}$  core and one valence neutron. This study includes calculations of complete fusion (CF) cross sections, systematically relaxing the rigid-body constraints on the nuclei involved in the collisions. Fusion cross sections for central collision have been calculated in (Katariya & Godre 2021). However, at higher energies, contributions from higher partial waves become significant and cannot be neglected. To address this, the CF cross-section is calculated for non-central collisions ( $b > 0$ ) in the present work.

In this paper, the details of the model are presented in model details Section, while the details and the results for fusion cross-sections for  $^{11}\text{Be} + ^{209}\text{Bi}$  are discussed in Fusion Cross-section Calculation Details. Finally, in last section conclusions are summarised.

## MODEL DETAILS

The  $^{11}\text{Be} + ^{209}\text{Bi}$  reaction is stimulated in the Multibody Three-Stage Classical Molecular Dynamics (3S-CMD) model. The projectile  $^{11}\text{Be}$  is constructed as a cluster of tightly bound  $^{10}\text{Be}$  and one neutron. Tightly bound  $^{10}\text{Be}$  and  $^{209}\text{Bi}$  are constructed using variational potential energy minimisation STATIC (Godre & Waghmare 1987) code and “cooled” using DYNAMIC (Godre & Waghmare 1987) code, for which a purely phenomenological softcore Gaussian potential is used, which is given by,

$$V_{ij}(r_{ij}) = -V_0 \left(1 - \frac{c}{r_{ij}}\right) \exp\left(-\frac{r_{ij}^2}{r_0^2}\right) \quad (1)$$

where the typical form of the Coulomb potential between protons is,

$$V_C(r_{ij}) = \frac{1.44}{r_{ij}} \text{ MeV} \quad (2)$$

and the potential parameter set  $V_0 = 710.0$  MeV,  $C = 1.88$  fm and  $r_0 = 1.15$  fm is used to produce ground state properties of nuclei. As some other weakly bound projectiles already constructed in (Morker, 2017) using a “dynamic cooling” method by carrying out rigid body dynamics like procedure and setting the cluster velocities and their angular moment zero after every time-step and thus obtaining the equilibrium orientation and position of the centre of mass of these constituents ( $^{10}\text{Be} + n$ ). Now, the distance between the centre of mass of  $^{10}\text{Be}$  and the neutron is adjusted in such a way that the typical ion-ion potential between them is equal to the experimental neutron separation energy of  $^{11}\text{Be}$ . Ground-state properties of generated nuclei are mentioned in Table 1.

In this multibody 3S-CMD model, there are three stages involved in the simulation:

(1) Rutherford Trajectories: The target and projectile are initially brought along classical Rutherford trajectories, considering their Coulomb interaction.

(2) Classical Rigid Body Dynamics (CRBD): The system evolves dynamically to approach the fusion barrier, incorporating collective motion and interactions.

(3) Classical Molecular Dynamics (CMD): The entire multibody system undergoes CMD evolution, allowing for interactions and dynamic evolution of the system.

In this model, for the first and second stages, the projectile and target are treated as complete rigid bodies, while during the third stage, this rigidity constraint on the target and projectile can be relaxed.

**Table 1: Ground-state properties.**

Nucleus	Calculated		Experimental	
	B.E. (MeV)	R (fm)	B.E.* (MeV)	R* (fm)
$^{10}\text{Be}$	59.68	2.09	65.97	2.28
$^{11}\text{Be}$ ( $^{10}\text{Be} + n$ )	60.18	2.06	65.55	2.90
$^{209}\text{Bi}$	1606.6	5.55	1640.26	5.52

(Wapstra & Bos 1977; Al-Khalili *et al.*, 1996; De Vries *et al.*, 1987)

The present study considers various assumptions regarding the rigid-body constraints on the projectile core,  $^{10}\text{Be}$ , and neutron, and the bond between them and the target nucleus,  $^{209}\text{Bi}$ . These assumptions/cases are detailed below:

**Case (a):** In this case, during Stage-3 of the model, the  $^{11}\text{Be}$  nucleus is kept completely rigid, with both its core,  $^{10}\text{Be}$  and neutron, treated as rigid, including the bond between them also to be rigid. The target nucleus,  $^{209}\text{Bi}$ , is considered non-rigid. This is denoted as:

$$^{11}\text{Be} [^{10}\text{Be}(\text{R}) - \text{R} - n] + ^{209}\text{Bi}(\text{NR})$$

**Case (b):** Here, in this case, for the  $^{11}\text{Be}$  nucleus, the  $^{10}\text{Be}$  core is treated rigid, but the bond between  $^{10}\text{Be}$  and the neutron is also kept non-rigid. The target nucleus,  $^{209}\text{Bi}$ , is considered non-rigid. This is denoted as:

$$^{11}\text{Be} [^{10}\text{Be}(\text{R}) - \text{NR} - n] + ^{209}\text{Bi}(\text{NR}).$$

For these cases large number of trajectories with Monte-Carlo sampled initial orientations are simulated for energies ranging from below the barrier to above the barrier energies, and fusion cross sections are calculated. Details of calculation of fusion cross section is given in next section.

## FUSION CROSS-SECTION CALCULATION DETAILS

Theoretically, the colliding nuclei are assumed to be fused when they overcome the potential barrier between them and become trapped in a potential pocket. In the present calculation, the fusion cross section for a given collision energy  $E_{\text{cm}}$  is calculated using Wong’s formula (Wong, 1973),

$$\sigma_{fus}(E_{CM}) = \left[ \frac{R_B^2 h \omega_0}{2E_{CM}} \right] \ln \left[ 1 + \exp \left( 2\pi \frac{(E_{CM} - V_B)}{h \omega_0} \right) \right] \quad (3)$$

Where  $V_B$ ,  $R_B$ , and  $\omega_0$  represent the barrier parameters. The fusion cross-section depends on how these barrier parameters are determined. The complete fusion cross section,  $\sigma_{\text{CF}}$  is defined as the capture of the total projectile charge. For head-on collisions ( $b=0$ ), the orientation-averaged fusion cross section is calculated by averaging over a large number of Monte Carlo-sampled initial orientations, spanning collision energies both above and below the barrier in (Katariya & Godre 2021) and is shown in Fig. 1.

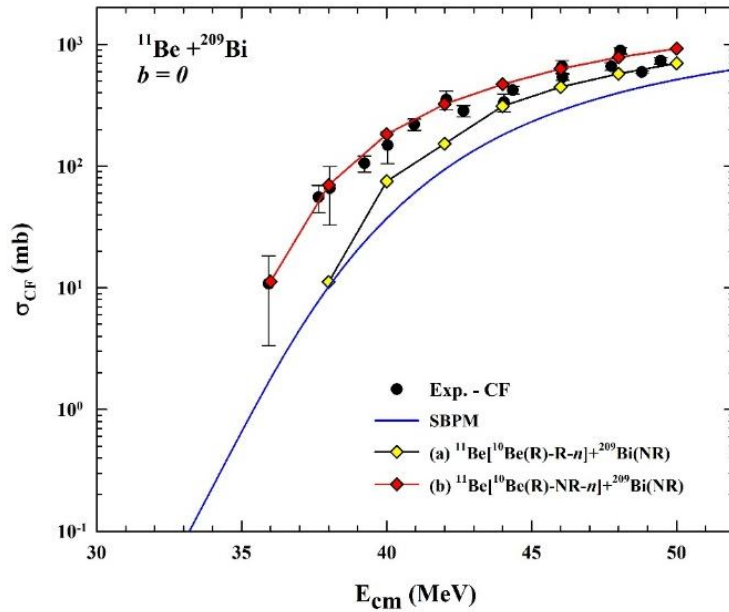


**Fig. 1.** for  $b=0$ ,  $\sigma_{CF}$  for  $^{11}\text{Be} + ^{209}\text{Bi}$  reaction with various assumptions of rigid body constraints for a projectile, the bond between them, and target. Exp.- CF (Signorini *et al.*, 2004).

The SBPM calculations, which neglect all dynamical effects, show highly suppressed fusion cross-sections. Systematically removing rigidity constraint on the target in 3S-CMD model calculations enhances the cross-section compared to SBPM but still deviates from experimental data. However, relaxing the bond between  $^{10}\text{Be}$  and the neutron in  $^{11}\text{Be}$  results in a significant cross-section enhancement, aligning well with experimental results.

However, the assumption of  $b = 0$  in Wong's formula is valid only at low energies. At higher energies, contributions from higher partial waves become

significant and cannot be neglected. To address this, the CF cross-section is also calculated for non-central collisions ( $b > 0$ ). The critical impact parameter for CF,  $b_{cr-CF}$ , is determined, and using the sharp cutoff approximation, it is assumed that all trajectories with  $b < b_{cr-CF}$  result in complete fusion, while those with  $b > b_{cr-CF}$  either lead to scattering or incomplete fusion (ICF). So, the CF cross section determined from  $b_{cr-CF}$  for cases (a) and (b) and shown in Fig. 2 where we find that  $\sigma_{CF}$  is enhanced compared to those shown in for  $b = 0$ .

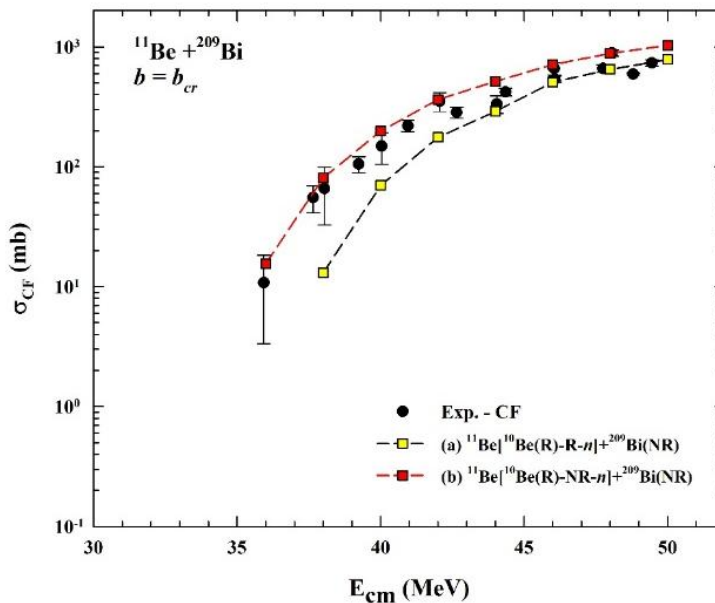


**Fig. 2.** for  $b=b_{cr}$ ,  $\sigma_{CF}$  for  $^{11}\text{Be} + ^{209}\text{Bi}$  reaction with various assumptions of rigid body constraints for a projectile, the bond between them, and target. Exp.- CF (Signorini *et al.*, 2004).

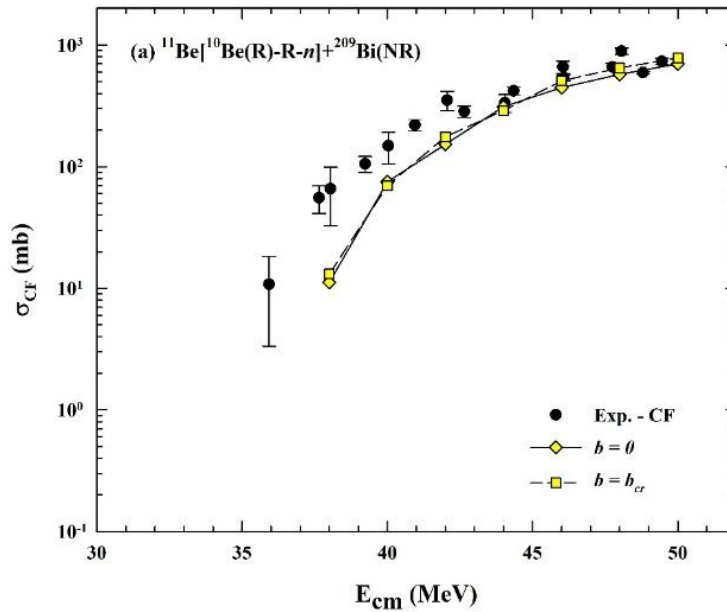


**Fig. 3.**  $\sigma_{CF}$  for  $^{11}\text{Be} + ^{209}\text{Bi}$  reaction: Case (a) for  $b=0$  and  $b=b_{cr}$  Exp.- CF (Signorini *et al.*, 2004).

Fig. 3 show the comparison of Fusion cross section for case (a) for central ( $b=0$ ) and noncentral ( $b_{cr}$ -CF) collisions. Fig. 4 show the comparison of Fusion cross section for case (b) for central ( $b=0$ ) and noncentral ( $b_{cr}$ -

CF) collisions. It can be clearly seen that impact parameter greatly influence the fusion outcomes and at critical impact parameter the complete fusion cross section enhances in both cases.

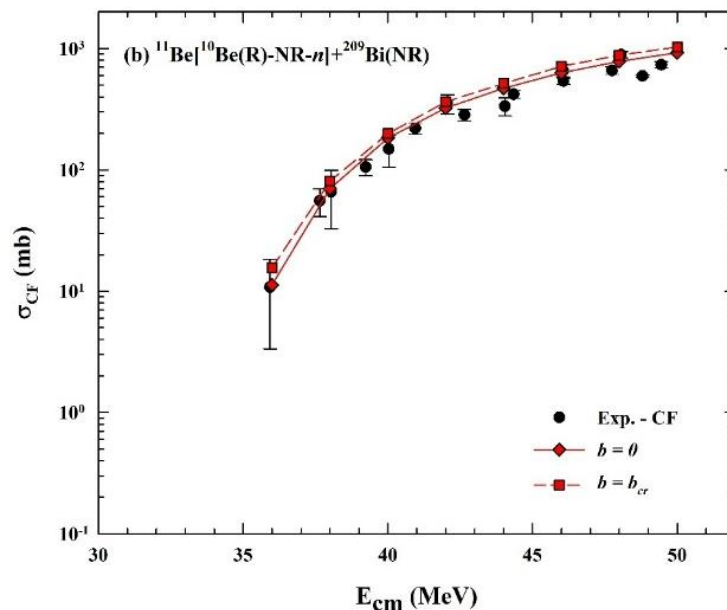


**Fig. 4.**  $\sigma_{CF}$  for  $^{11}\text{Be} + ^{209}\text{Bi}$  reaction: Case (b) for  $b=0$  and  $b=b_{cr}$ . Exp.- CF (Signorini *et al.*, 2004).

## CONCLUSIONS

The complete fusion (CF) cross-section,  $\sigma_{CF}$ , is significantly influenced by the rigidity constraints applied to both the target and the projectile. Using the multibody 3S-CMD model calculation for  $^{11}\text{Be} + ^{209}\text{Bi}$  reaction, the importance of incorporating various degrees of freedom in fusion cross section calculations is highlighted. Notably, the relaxation of the bond between the projectile core and the neutron results in a

substantial enhancement of the fusion cross-section. However, to account for the contribution of higher partial waves, fusion cross section is calculated at critical impact parameter which shows further enhancement of complete fusion cross sections compared to fusion cross section calculated for central collision for both the cases. Over all, with the multibody 3S-CMD model we can understand role of different parameters, offering better understanding of the fusion dynamics.

## REFERENCES

- Al-Khalili, J. S., Tostevin, J. A. & Thompson, I. J. (1996). Radii of halo nuclei from cross section measurements. *Physical review C*, 54(4), 1843.
- De Vries, H., De Jager, C. W. & De Vries, C. (1987). Nuclear charge-density-distribution parameters from elastic electron scattering. *Atomic data and nuclear data tables*, 36(3), 495-536.
- Duan, F. F., Yang, Y. Y., Wang, K., Moro, A. M., Guimarães, V., Pang, D. Y. & Xu, H. S. (2020). Scattering of the halo nucleus  $^{11}\text{Be}$  from a lead target at 3.5 times the Coulomb barrier energy. *Physics Letters B*, 811, 135942.
- Godre, S. S. & Waghmare, Y. R. (1987). Classical microscopic calculations of  $\text{O } 16+ \text{ }^{16}\text{O}$  and  $\text{Ca } 40+ \text{ }^{40}\text{Ca}$  fusion cross sections. *Physical Review C*, 36(4), 1632.
- Katariya, V. B. & Godre, S. S. (2021).  $^{11}\text{Be}$  (One-neutron halo)+  $^{209}\text{Bi}$  reaction in multi-body three-stage Classical Molecular Dynamics model. In Proceedings of the DAE Symp. on Nucl. Phys (Vol. 65, p. 315).
- Kobayashi, T., Shimoura, S., Tanihata, I., Katori, K., Matsuta, K., Minamisono, T. & Wieman, H. (1989). Electromagnetic dissociation and soft giant dipole resonance of the neutron-dripline nucleus  $^{11}\text{Li}$ . *Physics Letters B*, 232(1), 51-55.
- Kobayashi, T., Yamakawa, O., Omata, K., Sugimoto, K., Shimoda, T., Takahashi, N. & Tanihata, I. (1988). Projectile Fragmentation of the Extremely Neutron-Rich Nucleus  $^{11}\text{Li}$  at 0.79 GeV/nucleon. *Physical Review Letters*, 60(25), 2599.
- Morker, M. R. (2017). Study of effects of weakly bound projectile breakup on heavy-ion fusion (Doctoral dissertation). Veer Narmad South Gujarat University, Surat.
- Signorini, C., Yoshida, A., Watanabe, Y., Pierrousakou, D., Stroe, L., Fukuda, T. & Hagino, K. (2004). Subbarrier fusion in the systems  $^{11}\text{B}+ \text{ }^{209}\text{Bi}$ . *Nuclear Physics A*, 735(3-4), 329-344.
- Tanihata, I., Hamagaki, H., Hashimoto, O., Nagamiya, S., Shida, Y., Yoshikawa, N. & Nojiri, Y. (1985). Measurements of interaction cross sections and radii of He isotopes. *Physics Letters B*, 160(6), 380-384.
- Tanihata, I., Hamagaki, H., Hashimoto, O., Shida, Y., Yoshikawa, N., Sugimoto, K. & Takahashi, N. (1985). Measurements of interaction cross sections and nuclear radii in the light p-shell region. *Physical Review Letters*, 55(24), 2676.
- Wapstra, A. H. & Bos, K. (1977). The 1977 atomic mass evaluation: in four parts part I. Atomic mass table. *Atomic Data and Nuclear Data Tables*, 19(3), 177-214.
- Wong, C. (1973). Interaction barrier in charged-particle nuclear reactions. *Physical Review Letters*, 31(12), 766.

**How to cite this article:** V.B. Katariya and P.H. Jariwala (2025). Fusion Cross Section for Non-central Collision in  $^{11}\text{Be} + ^{209}\text{Bi}$  Reaction using Multi-body Three-Stage Classical Molecular Dynamics Approach. *International Journal of Theoretical & Applied Sciences*, 17(1): 75–79.